Broad-Band Analysis of a Coaxial Discontinuity Used for Dielectric Measurements

NOUR-EDDINE BELHADJ-TAHAR AND ARLETTE FOURRIER-LAMER

Abstract—**A coaxial line terminated by a gap is considered, the gap being filled with an unknown material. This cell enables measurements of complex permittivity of dielectric materials to be made. The relationship linking the measured admittance to the dielectric properties is obtained from a theoretical analysis of the electromagnetic field in the line. The equivalent-circuit parameters of a coaxial line terminated by a gap are obtained; all higher order waves excited at the discontinuity are taken into account. The measurements show good agreement between measured and calculated data from dc to 12.4 GHz.**

I. Introduction

THE GEOMETRY OF this problem, composed of a junction of a coaxial guide and a short circular guide, is shown in Fig. 1.

N. Marcuvitz [1] found an approximate solution by using the small-aperture method treating all higher modes by plane parallel approximations. The proposed equivalent circuit is an approximation valid for $d/(a-b)$[1] and $2\pi d/\lambda \ll 1$. The discontinuity admittance appearing at the plane of discontinuity is capacitive and is valid at least so long as frequency is below the value for which the spacing between conductors of the coaxial line is a half wavelength. H. E. Green [2] and L. Young [3] have treated numerically this problem for very low frequencies. A least-squares boundary residual method has been used by R. Jansen [4] for the numerical solution of the discontinuity admittance.

This paper presents a general formulation. The problem is treated by the mode-matching method in which the fields on each side of discontinuity are expanded in an infinite series of modes matched across the boundary to preserve continuity. This was the approach used by Whinnery and his coworkers [5] in the analysis of a sudden change in diameter of the inner conductor of coaxial lines.

The solution of the field equation yields the equivalent admittance without any restrictions.

II. Formulation of the Gap Problem

To illustrate the formulation of the gap problem, let us consider the geometry shown in Fig. 1. The structure consists of an interruption of the inner conductor of the coaxial line. The A region is filled by air, while the B region is filled by an isotropic and nonmagnetic material with complex permittivity $\epsilon_0\epsilon^*$. The conductors of the line are assumed perfect for present purposes.

A study of the discontinuity shows then that field components E_r, E_z, and H_ϕ are required. Thus, in addition to the principal wave in the A region (TEM field), higher order waves of the transverse magnetic type (E waves) are excited at the plane of discontinuity ($z = 0$).

In the A region, the modal expansions for the transverse components of the electric and magnetic fields are

$$E_{r_A} = \frac{1}{r} A_0 [\exp jk_0 z + \Gamma \exp - jk_0 z] + \sum_m A_m Z_1(k_{A_m} r) \exp - \gamma_m \cdot z$$

$$H_{\phi_A} = \frac{1}{r} Y_{A_0} A_0 [\exp jk_0 z - \Gamma \exp - jk_0 z] + \sum_m A_m \cdot Y_{A_m} Z_1(k_{A_m} r) \exp - \gamma_m \cdot z \qquad (1)$$

where $\Gamma = A_0'/A_0$ is the reflection coefficient at $z = 0$, and A_0' and A_0 are the amplitudes of the reflected and incident TEM waves, respectively

$$Y_{A_0} = -\sqrt{\frac{\epsilon_0}{\mu_0}} \quad Y_{A_m} = \frac{j\omega\epsilon_0}{\gamma_m}$$

$$\gamma_m = k_{A_m}\sqrt{1-(k_0/k_{A_m})^2} \quad \text{and} \quad k_0 = \omega\sqrt{\mu_0\epsilon_0}. \qquad (2)$$

In the above, Z_p denotes the linear combination of pth order Bessel functions of the first and second kinds

$$Z_p(k_{A_m} \cdot r) = J_p(k_{A_m} \cdot r) + G_{A_m} \cdot N_p(k_{A_m} \cdot r). \qquad (3)$$

The required boundary condition on the electric field at the short circuit $z = -d$ gives the solutions for the B region

$$E_{r_B} = \sum_n B_n' J_1(k_{B_n} \cdot r) sh\gamma_n(z+d)$$

$$H_{\phi_B} = \sum_n \frac{-j\omega\epsilon_0\epsilon^*}{\gamma_n} B_n' J_1(k_{B_n} \cdot r) ch\gamma_n(z+d) \qquad (4)$$

where

$$\gamma_n = k_{B_n}\sqrt{1-(k_0\sqrt{\epsilon^*}/k_{B_n})^2} \quad \text{and} \quad \epsilon^* = \epsilon' - j\epsilon''.$$

Manuscript received July 22, 1985; revised October 18, 1985.

The authors are with the Laboratoire de Dispositifs Infrarouge (UA CNRS 836), Université Pierre et Marie Curie, Tour 12, 4 place Jussieu 75230 Paris Cedex 05, France.

IEEE Log Number 8406859.

0018-9480/86/0300-0346$01.00 ©1986 IEEE

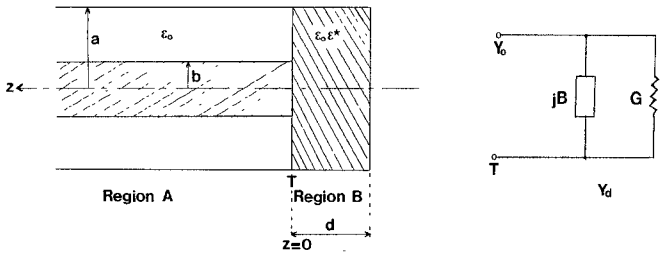

Fig. 1. Geometry of the gap.

The boundary conditions at the conductors of the line require that E_z is zero for each E wave at $r = a$ and $r = b$ in the A region, and $r = a$ at the B region. Then

$$Z_0(k_{A_m} \cdot a) = Z_0(k_{A_m} \cdot b) = 0 \tag{5}$$

$$J_0(k_{B_n} \cdot a) = 0 \tag{6}$$

and from the definition of (3) and (5) requires

$$G_{A_m} = -\frac{J_0(k_{A_m} \cdot a)}{N_0(k_{A_m} \cdot a)} = -\frac{J_0(k_{A_m} \cdot b)}{N_0(k_{A_m} \cdot b)} \tag{7}$$

$$J_0(k_{A_m} \cdot a) \cdot N_0(k_{A_m} \cdot b) - J_0(k_{A_m} \cdot b) \cdot N_0(k_{A_m} \cdot a) = 0. \tag{8}$$

The required matching conditions at the reference plane $z = 0$ are

$$E_{r_B} = 0 \quad 0 < r < b \tag{9}$$

$$Er_B = \sum_n B_n J_1(k_{B_n} \cdot r) = \frac{1}{r} A_0(1+\Gamma) + \sum_m A_m Z_1(k_{A_m} \cdot r), \quad b < r < a \tag{10}$$

$$H_{\phi_B} = \sum_n B_n Y_{B_n} J_1(k_{B_n} \cdot r) = \frac{1}{r} Y_{A_0} A_0(1-\Gamma) + \sum_m A_m Y_{A_m} Z_1(k_{A_m} \cdot r), \quad b < r < a \tag{11}$$

where $B_n = B_n' sh\gamma_n d$ and

$$\gamma_{B_n} = \frac{-j\omega\epsilon_0\epsilon^*}{k_{B_n}\sqrt{1-\left(k_0\sqrt{\epsilon^*}/k_{B_n}\right)^2}} \cdot \coth\left[k_{B_n}\sqrt{1-\left(k_0\sqrt{\epsilon^*}/k_{B_n}\right)^2}\, d\right]. \tag{12}$$

The coefficients in (10) and (11) are determined by using the orthogonality properties of Bessel functions. The first step is to perform the following integral:

$$\int_0^a r \cdot J_1(k_{B_q} \cdot r) E_{r_B}\, dr. \tag{13}$$

Applying the Lommel integrals with (9), (10, (5), and (6), one may write

$$\frac{B_n}{k_{B_n} A_0(1+\Gamma)} = \frac{2J_0(k_{B_n} \cdot b)}{\left[k_{B_n} \cdot aJ_1(k_{B_n} \cdot a)\right]^2} \cdot \left[1 - b \cdot \sum_m \frac{A_m}{A_0(1+\Gamma)} \cdot \frac{Z_1(k_{A_m} \cdot b)}{(k_{A_m}/k_{B_n})^2 - 1}\right]. \tag{14}$$

Now H_{ϕ_B} is integrated over the range $b < r < a$. Recalling (11), (5), (6), and the property of Bessel functions

$$\int Z_1(k \cdot r)\, dr = -\frac{1}{k} Z_0(k \cdot r)$$

one obtains

$$Y_{A_0} A_0(1-\Gamma) \ln\frac{a}{b} = \sum_n \frac{B_n Y_{B_n}}{k_{B_n}} \cdot J_0(k_{B_n} \cdot b). \tag{15}$$

The last step is to integrate the quantity $rZ_1(k_{A_p} \cdot r) H_{\phi_B}$ over the range $b < r < a$. Then

$$\frac{Y_{A_p} \cdot A_p}{2} \cdot \left\{\left[a \cdot Z_1(k_{A_p} \cdot a)\right]^2 - \left[b \cdot Z_1(k_{A_p} \cdot b)\right]^2\right\} = \sum_n \frac{B_n Y_{B_n} k_{B_n} \cdot bJ_0(k_{B_n} \cdot b) Z_1(k_{A_p} \cdot b)}{k_{B_n}^2 - k_{A_p}^2}. \tag{16}$$

The normalized admittance Y_d/Y_0 may be written in the following form: $Y_d/Y_0 = (1-\Gamma)/(1+\Gamma)$. Incorporating (14) into (15) allows us to derive the following solution:

$$\frac{Y_d}{Y_0} = j\frac{k_0\epsilon^*}{\ln\frac{a}{b}} \cdot \sum_n \frac{2J_0^2(k_{B_n} \cdot b)\coth\left[k_{B_n}\sqrt{1-\left(k_0\sqrt{\epsilon^*}/k_{B_n}\right)^2}\, d\right]}{k_{B_n}\sqrt{1-\left(k_0\sqrt{\epsilon^*}/k_{B_n}\right)^2} \cdot \left[k_{B_n} \cdot aJ_1(k_{B_n} \cdot a)\right]^2} \cdot \left[1 - b\sum_m \frac{A_m}{A_0(1+\Gamma)} \cdot \frac{Z_1(k_{A_m} \cdot b)}{(k_{A_m}/k_{B_n})^2 - 1}\right]. \tag{17}$$

III. Numerical Computation

The computation of (17) starts with the evaluation of quantities derived from Bessel functions. A Bessel subroutine calculates the zero and first-order Bessel functions of the first and second kinds (J_0, J_1, N_0, N_1). For these orders, the routine is accurate down to the smallest practical arguments. The accuracy is generally to five decimal places. If large arguments are required, the standard trigonometric approximations are applicable. The roots of the transcendental equations (6) and (8) are found by iteration. It can be shown that all these roots (k_{Am}, k_{Bn}) are real even in the lossy case (lossy materials in the B region) and so, the arguments of the calculated Bessel functions are real. From the desired number of roots, the quantities k_{Am}, k_{Bn}, and finally the values of Z_i are obtained.

For dielectric materials of known properties, the first part of the summation in (17) may be calculated at once.

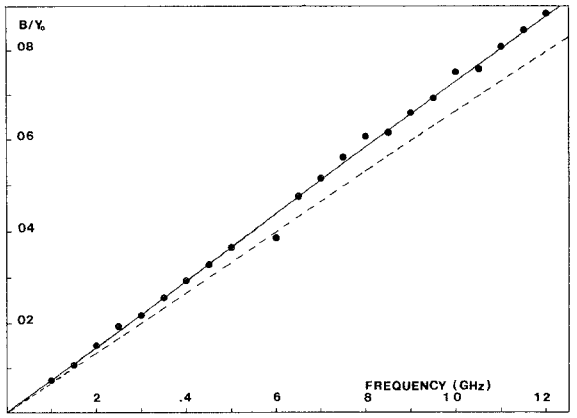

Fig. 2. Admittance of the General Radio cell filled by air; $d = 2$ mm. (●): Experimental data. ——: This theory. ----: Marcuvitz formula.

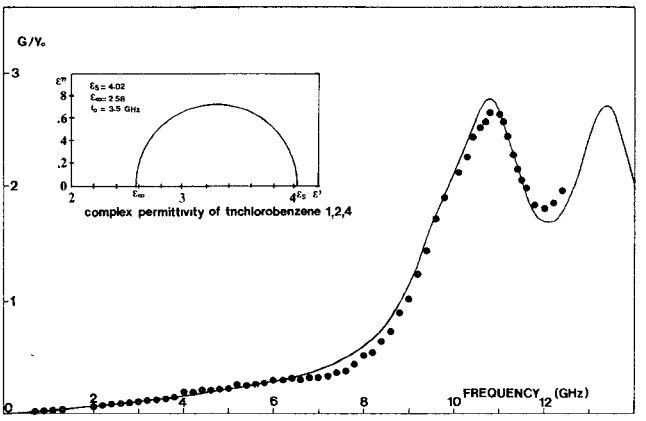

Fig. 4 Variation of the real part of the cell's admittance filled with trichlorobenzene 1,2,4. Cell: General Radio; $d = 20.45$ mm.

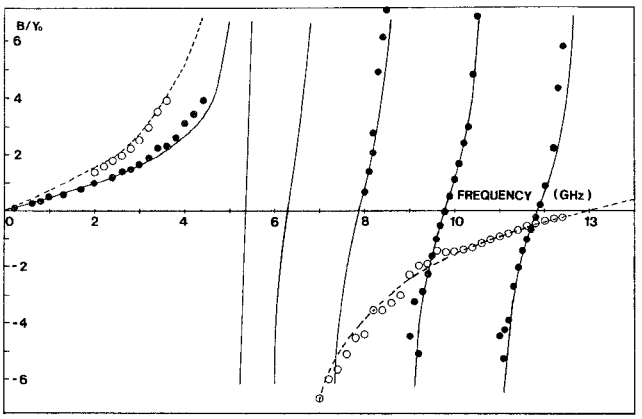

Fig. 3. Admittance of the General Radio cell filled with alumina. ——: Theoretical ($d = 20.45$ mm; $\epsilon' = 9.6$). (●): Experimental data. ----: Theoretical ($d = 2$ mm; $\epsilon' = 9.6$). (○): Experimental data.

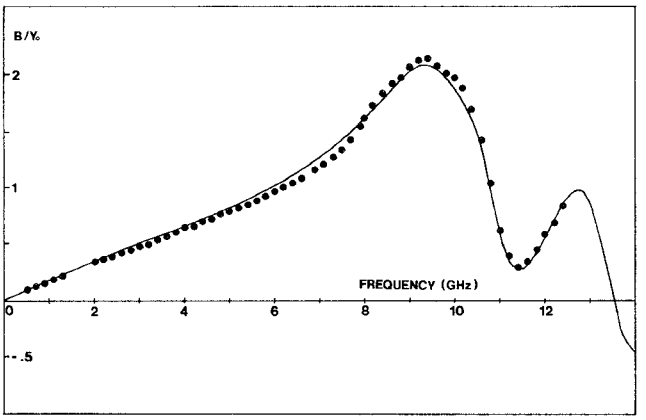

Fig. 5. Variation of the imaginary part of the cell's admittance filled with trichlorobenzene 1,2,4. Cell: General Radio; $d = 20.45$ mm.

The coefficients $A_m/[A_0(1+\Gamma)]$ are obtained by (16) using (14), (12), and (2).

$$\frac{A_p}{2k_{A_p}\sqrt{1-(k_0/k_{A_p})^2}}\left\{\left[aZ_1(k_{A_p}\cdot a)\right]^2-\left[bZ_1(k_{A_p}\cdot b)\right]^2\right\}$$
$$= -\epsilon^* A_0(1+\Gamma)\cdot\sum_n \frac{2J_0^2(k_{B_n}\cdot b)k_{B_n}\cdot bZ_1(k_{A_p}\cdot b)\coth\left[k_{B_n}\alpha_n d\right]}{\alpha_n\left[k_{B_n}\cdot aJ_1(k_{B_n}\cdot a)\right]^2\left[k_{B_n}^2-k_{A_p}^2\right]}\cdot\left[1-b\sum_m \frac{A_m}{A_0(1+\Gamma)}\cdot\frac{Z_1(k_{A_m}\cdot b)}{(k_{A_m}/k_{B_n})^2-1}\right] \quad (18)$$

where $\alpha_n = 1-(k_0\sqrt{\epsilon^*}/k_{B_n})$. One obtains

The solutions of the above matrix equation are obtained by retaining a finite number of higher order modes.

IV. Numerical Results and Experimental Verifications

The numerical results for the homogeneous case have been checked against experiment by measuring the discontinuity admittance versus frequency for the gap filled by air. The measurements have been made by the microwave automatic analyzer HP 8410B and are shown in Fig. 2. In the same figure, comparison is made with the Marcuvitz formula. Measurements have also been made for alumina both with $d = 20.45$ mm and $d = 2$ mm. Results and comparison with theory are shown in Fig. 3. Figs. 4 and 5 represent measurements on trichlorobenzene 1,2,4. Trichlorobenzene is assumed lossy with the following complex permittivity (Debye relation) represented by the Argand

$$\frac{A_p}{A_0(1+\Gamma)}\cdot\frac{\left[k_{A_p}\cdot aZ_1(k_{A_p}\cdot a)\right]^2-\left[k_{A_p}\cdot bZ_1(k_{A_p}\cdot b)\right]^2}{4k_{A_p}\sqrt{1-(k_0/k_{A_p})^2}\,Z_1(k_{A_p}\cdot b)} = \epsilon^*\sum_n \frac{k_{B_n}\cdot bJ_0^2(k_{B_n}\cdot b)\coth\left[k_{B_n}\alpha_n d\right]}{\alpha_n\left(1-k_{B_n}^2/k_{A_p}^2\right)\left[k_{B_n}\cdot aJ_1(k_{B_n}\cdot a)\right]^2}$$
$$-\epsilon^*\sum_m \frac{A_m}{A_0(1+\Gamma)}\frac{Z_1(k_{A_m}\cdot b)}{k_{A_m}^2\cdot b}\cdot\sum_n \frac{(k_{B_n}\cdot b)^3J_0^2(k_{B_n}\cdot b)\coth\left[k_{B_n}\alpha_n d\right]}{\alpha_n\left(1-k_{B_n}^2/k_{A_p}^2\right)\left(1-k_{B_n}^2/k_{A_m}^2\right)\left[k_{B_p}\cdot aJ_1(k_{B_n}\cdot a)\right]^2}. \quad (19)$$

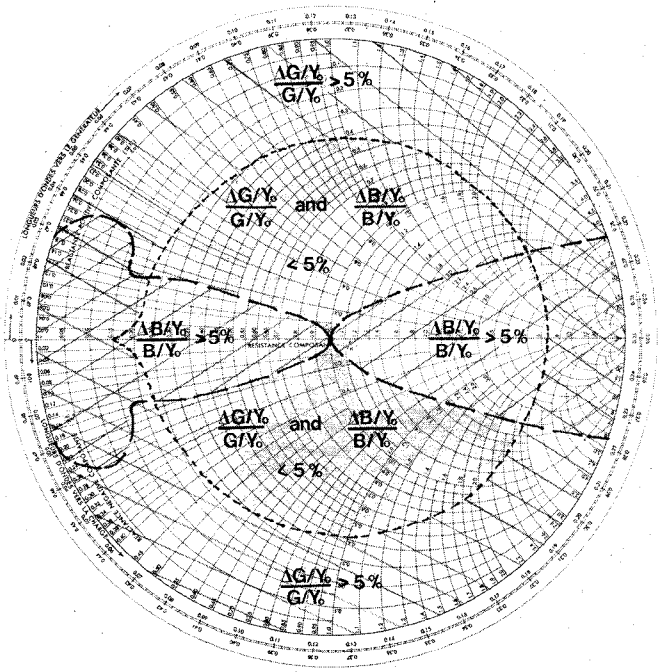

Fig. 6. Example of the accuracy of measurements.

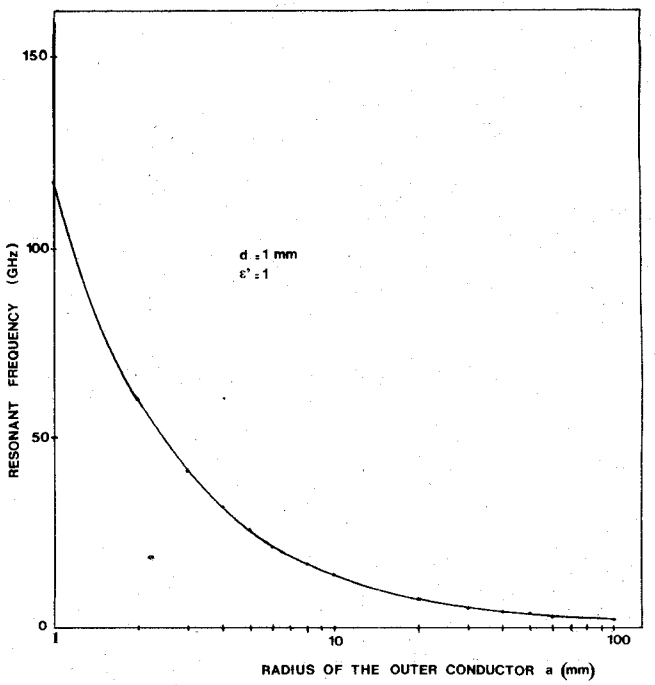

Fig. 7. Theoretical resonant frequency of the gap in a 50-Ω line.

diagram in the inset in Fig. 4:

$$\epsilon^* = \epsilon_\infty + (\epsilon_S - \epsilon_\infty)/(1 + jf/f_0)$$

where $\epsilon_s = 4.02$, $\epsilon_\infty = 2.58$, and $f_0 = 3.5$ GHz. The accuracy of measurements depends on the measured values of B/Y_0 and G/Y_0. An example of the accuracy provided by the automatic network analyzer is graphed in Fig. 6. It is interesting to note that values of B/Y_0 or G/Y_0 less than 10^{-3} or more than 10^3 involve, generally, errors greater than 100 percent in the corresponding values. This is the case of dielectric samples with too small losses (the measured values of G/Y_0 are not available, viz, alumina) and of values near the resonant frequency.

The first resonant frequency occurs when the fundamental TM_{01} mode is above its cutoff frequency. For the lossless case, the value of this resonant frequency is obtained by (19), setting $\Gamma = -1$. It should be pointed out that the first resonant frequency depends on a, b, ϵ', and d and tends to the cutoff frequency of the TM_{01} mode for large values of d. Thus, to avoid prohibitive experimental values, the radius of the outer conductor is reduced (Fig. 7): 50 Ω − APC7-mm line ($a = 3.5$ mm) is used up to 18 GHz. The other resonant frequencies are given by

$$f_q = \frac{c}{\sqrt{\epsilon'}} \left(\frac{q^2}{4d^2} + \frac{k_{B_1}^2}{4\pi^2} \right)^{1/2}, \qquad q = 1, 2, 3 \cdots .$$

The gap behaves then as a resonant cavity where the TM_{01} is stationary.

V. The Inverse Problem

To deduce the complex permittivity from the measurements of the admittance Y_d/Y_0, an iterative method is used. Broad-band dielectric investigations on several materials have been made. Now, electroactive polymers are studied by this method. The results have shown that the complex permittivity can be measured with an error of less than 5 percent by proper choice of sample dimensions. This work will be published in a future paper.

VI. Conclusions

An approach for computing the equivalent-circuit parameters for the termination of a coaxial line by a gap filled by lossy materials is described. The method is quite general and the results show that the analysis is accurate over a broad range of frequencies. This cell enables measurements of the complex permittivity of dielectric materials to be made.

References

[1] N. Marcuvitz, *Waveguide Handbook*, 1st Ed. New York, McGraw-Hill, 1951, sec. 5, ch. 4, p. 178.
[2] H. E. Green, "The numerical solution of some important transmission line problems," *IEEE Trans. Microwave Theory Tech.*, vol. MTT-13, pp. 676–692, Sept. 1965.
[3] L. Young, "The practical realization of series-capacitive couplings for microwave filters," *Microwave J.*, vol. 5, p. 79, Dec. 1962.
[4] R. Janssen, "On the performance of the least squares method for waveguide junctions and discontinuities," *IEEE Trans. Microwave Theory Tech.*, vol. MTT-23, pp. 434–436, May 1975.
[5] J. R. Whinnery, H. W. Jamieson, and T. E. Robbins, "Coaxial line discontinuities," *Proc. IRE*, vol. 32, pp. 695–709, Nov. 1944.

✠

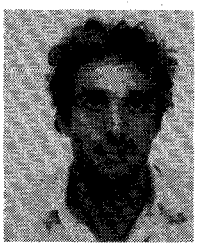

Nour-Eddine Belhadj-Tahar was born in Tlemcen, Algeria, on September 23, 1954. He received the Dipl.-Ing. degree in electrical engineering from the University of Sciences and Technology of Oran, Algeria, in 1977.

From September 1980 to June 1982, he was an Assistant Professor in the Institute of Physics, University of Tlemcen, Algeria. In 1983, he received the "Diplôme d'études approfondies" (DEA) in electrical engineering from the University Pierre et Marie Curie, Paris, France. He is

now preparing a Doctorat thesis at the University Pierre et Marie Curie, Paris, on microwave techniques for dielectric measurements.

✠

Arlette Fourrier-Lamer received the Ph.D. (Doctorat d'Etat és Sciences Physiques) from the University Pierre et Marie Curie, in 1981.

Up to this date, she has been engaged in research on electron and nuclear double resonance (ENDOR) in paramagnetic liquids. Since 1982, she has been working on dielectric measurements of polymers for electrical engineering of microwave systems. She is Assistant Professor in the University of Pierre et Marie Curie, where she teaches microwave circuits.

Dr. Fourrier-Lamer is a member of the Societé Française des Electroniciens et des Radioélectriciens (S.E.E.).